⌘ *Author's Choice*

THE JOURNAL OF BIOLOGICAL CHEMISTRY VOL. 285, NO. 26, pp. 19720–19726, June 25, 2010

The E3 Ubiquitin Ligase IDOL Induces the Degradation of the Low Density Lipoprotein Receptor Family Members VLDLR and ApoER2*[S]

Received for publication, March 15, 2010, and in revised form, April 27, 2010 Published, JBC Papers in Press, April 28, 2010, DOI 10.1074/jbc.M110.123729

Cynthia Hong[‡1], Sarah Duit[§1], Pilvi Jalonen[¶1], Ruud Out[‖], Lilith Scheer[**], Vincenzo Sorrentino[**], Rima Boyadjian[‡], Kees W. Rodenburg[‡‡], Edan Foley[§§2], Laura Korhonen[¶], Dan Lindholm[¶¶3], Johannes Nimpf[§4], Theo J. C. van Berkel[‖], Peter Tontonoz[‡5], and Noam Zelcer[‖6]**

*From the [‡]Department of Pathology and Laboratory Medicine and the Howard Hughes Medical Institute, University of California, Los Angeles, California 90095, the [§]Max F. Perutz Laboratory, Department of Medical Biochemistry, Medical University of Vienna, A-1030 Vienna, Austria, the [¶]Minerva Medical Research Institute, Biomedicum-2, 00290 Helsinki, Finland, the [‖]Division of Biopharmaceutics, Leiden Amsterdam Center for Drug Research, University of Leiden, 2300RA Leiden, The Netherlands, the [§§]Department of Medical Microbiology and Immunology, University of Alberta, Edmonton, Alberta T6G 2S2, Canada, the [‡‡]Division of Endocrinology and Metabolism, Department of Biology, University of Utrecht, 3584 CH Utrecht, The Netherlands, the [¶¶]Institute of Biomedicine/Biochemistry, University of Helsinki, 00014 Helsinki, Finland, and the **Department of Medical Biochemistry, Academic Medical Center, University of Amsterdam, 1105 AZ Amsterdam, The Netherlands*

We have previously identified the E3 ubiquitin ligase-inducible degrader of the low density lipoprotein receptor (LDLR) (Idol) as a post-translational modulator of LDLR levels. Idol is a direct target for regulation by liver X receptors (LXRs), and its expression is responsive to cellular sterol status independent of the sterol-response element-binding proteins. Here we demonstrate that Idol also targets two closely related LDLR family members, VLDLR and ApoE receptor 2 (ApoER2), proteins implicated in both neuronal development and lipid metabolism. Idol triggers ubiquitination of the VLDLR and ApoER2 on their cytoplasmic tails, leading to their degradation. We further show that the level of endogenous VLDLR is sensitive to cellular sterol content, Idol expression, and activation of the LXR pathway. Pharmacological activation of the LXR pathway in mice leads to increased Idol expression and to decreased Vldlr levels *in vivo*. Finally, we establish an unexpected functional link between LXR and Reelin signaling. We demonstrate that LXR activation results in decreased Reelin binding to VLDLR and reduced Dab1 phosphorylation. The identification of VLDLR and ApoER2 as Idol targets suggests potential roles for this LXR-inducible E3 ligase in the central nervous system in addition to lipid metabolism.

The LDLR[7] family of membrane receptors consists of type I membrane proteins that participate in endocytic and cellular signaling processes. The LDLR, the namesake of the family, is essential for the uptake of extracellular LDL cholesterol (1). As such, it is a critical determinant of plasma lipoprotein levels and a target for human cardiovascular therapeutics. Mutations in this receptor are the leading cause of familial hypercholesterolemia, a disease characterized by reduced hepatic LDL clearance, elevated plasma cholesterol levels, and accelerated cardiovascular disease (2–4).

Expression of the LDLR is tightly regulated at both the transcriptional and post-transcriptional levels. Transcription of the *LDLR* gene is regulated primarily by sterol response element-binding protein (SREBP) transcription factors whose activity is sensitive to endoplasmic reticulum cholesterol levels (5, 6). A reduction in cellular cholesterol levels leads to the processing of SREBPs to their mature nuclear forms and the subsequent activation of genes important for cholesterol uptake and *de novo* cholesterol synthesis (7). Mechanisms for post-translational modulation of the LDLR pathway include LDLR adaptor protein 1 (*LDLRAP1/ARH*) (8) and *PCSK9* (proprotein convertase subtilisin/kexin 9) (9–12), which influence LDLR stability, endocytosis, and trafficking.

We have recently identified the E3 ubiquitin ligase Idol (inducible degrader of the LDLR) as a transcriptional target of LXRs and a post-transcriptional regulator of the LDLR pathway (13). Unlike the *LDLR* and *PCSK9* genes, *Idol* is not regulated by SREBPs. Therefore, LXR-dependent induction of Idol defines a complementary but distinct pathway for sterol-dependent inhibition of cellular cholesterol uptake through the LDLR. Idol triggers ubiquitination of the LDLR on conserved residues in its intracellular tail, leading to degradation of the receptor. Con-

* This work was supported, in whole or in part, by National Institutes of Health Grants HL066088 and HL090553 (to P. T.).
⌘ *Author's Choice*—Final version full access.
[S] The on-line version of this article (available at http://www.jbc.org) contains supplemental Figs. S1–S6.
[1] These authors contributed equally to this work.
[2] Supported by the Canadian Institutes of Health Research. Alberta Heritage Foundation for Medical Research Scholar. Canada Research Chair in Innate Immunity.
[3] Supported by grants from the Academy of Finland and the Sigrid Juselius Foundation.
[4] Supported by the Fonds zur Förderung der Wissenschaftlichen Forschung and the Herzfelder'sche Familienstiftung.
[5] Investigator of the Howard Hughes Medical Institute.
[6] Supported by a Career Development Award from the Human Frontier Science Program Organization and by a VIDI grant from the Netherlands Organization for Scientific Research (NWO). To whom correspondence should be addressed: Meibergdreef 15, 1105 AZ Amsterdam, The Netherlands. Tel.: 31-20-566-5131; Fax: 31-20-6915519; E-mail: n.zelcer@amc.uva.nl.

[7] The abbreviations used are: LDLR, low density lipoprotein receptor; ApoER2, ApoE receptor 2; LXR, liver X receptors; APP, amyloid precursor protein; E3, ubiquitin-protein isopeptide ligase; CNS, central nervous system; SREBP, sterol response element-binding protein; GFP, green fluorescent protein; HA, hemagglutinin.

sistent with this mechanism, overexpression of Idol potently reduces LDLR protein levels *in vitro* and *in vivo* and inhibits LDL uptake. Conversely, knockdown of Idol expression leads to an increase in LDLR protein and LDL uptake.

Among the LDLR family of proteins, the VLDLR (very low density lipoprotein receptor) and ApoER2 (also known as LRP8) share the highest overall sequence homology with the LDLR (14). Whereas the metabolic role of the LDLR is well established, study of the metabolic roles of VLDLR and ApoER2 has been complicated by the overlapping substrate specificity of LDLR family members (15). On the other hand, studies in recent years have established a critical role for VLDLR and ApoER2 in the neuronal Reelin pathway that is essential for proper neuronal positioning and brain development (16–19). A body of evidence demonstrates that the VLDLR and ApoER2 interact with an extracellular ligand, Reelin, leading, as a first event, to phosphorylation of the adaptor molecule Dab1 (20, 21).

In this study, we identify the VLDLR and ApoER2 as novel targets of Idol. Similar to the LDLR, these receptors are targeted by Idol for degradation through a post-translational mechanism dependent on the ubiquitination of conserved residues in their intracellular tail (13). We further show that the function of Idol is evolutionarily conserved and that the level of endogenous VLDLR is sensitive to cellular sterol levels and LXR activation both *in vitro* and *in vivo*. Finally, we provide evidence of cross-talk between the LXR-Idol pathway and Reelin signaling. Our findings suggest that Idol may have a role in the CNS in addition to its role in lipid metabolism.

EXPERIMENTAL PROCEDURES

Cell Culture, Transfections, and Adenoviral Infection—HEK 293T cells were from the ATCC. HEK 293T-Reelin cells were a gift from Dr. Thomas Curran (Children's Hospital of Philadelphia). SNB-19 glioblastoma cells were a gift from Dr. Rene Bernards (The Netherlands Cancer Institute, Amsterdam, The Netherlands). The generation and maintenance of 3T3 mouse fibroblasts that stably produce VLDLR and Dab1 were previously reported (22). The cells were maintained in Dulbecco's modified Eagle's medium (Invitrogen) supplemented with 10% fetal bovine serum at 37 °C and 5% CO_2. To collect Reelin-containing conditioned medium, HEK 293T-Reelin cells were grown to ~75% confluence, washed twice with phosphate-buffered saline and cultured in Optimem medium (Invitrogen) for an additional 24 h. Conditioned medium was collected, filtered, and stored at −80 °C. HEK 293T cells were transfected with Lipofectamine 2000 (Invitrogen) according to the manufacturer's instructions. In experiments testing the ability of Idol to degrade other potential protein targets, a ratio of 3:1 (IDOL: target) was used. The generation of adenoviruses encoding Idol, GFP, and Sult2b1 was previously described (13, 23). SNB-19 cells were seeded (0.5×10^6 cells/60-mm well) and infected with adenovirus the following day at a multiplicity of infection of 80. Primary hippocampal neurons were prepared from embryonic 17-day-old rats and cultured as described (24).

Plasmids and Expression Constructs—Expression plasmids for human IDOL, mouse Idol, HA-ubiquitin, LDLR, and LpR were previously reported (13, 25). The C-terminally tagged VLDLR-HA, VLDLR-GFP, and ApoER2-HA expression constructs were gifts from Dr. George Rebeck (Georgetown University). The FLAG-Lrp1b expression plasmid was a gift from Dr. Masashi Kawaichi (Nara Institute of Science and Technology, Japan). Full-length *Drosophila melanogaster* Dnr1 was cloned into the gateway plasmid pDONR221 (Invitrogen). To generate mammalian expression constructs for Dnr1, we used LR recombination between pDONR221-Dnr1 and an N-terminally V5 tag DEST plasmid (Invitrogen). Site-directed mutagenesis was used to introduce mutations in VLDLR-HA and V5-Dnr1 with the QuikChange multi-site mutagenesis kit (Stratagene). An amyloid precursor protein (APP) chimeric construct, $N'\text{-APP}_{(1-675)}\text{-LDLR}_{(780-860)}\text{-}C'$, that contains the APP ectodomain and the transmembrane and intracellular domains of the LDLR fused to a C-terminal GFP was generated by standard cloning procedures. Restriction digest analysis and DNA sequencing were used to verify the correctness of all of the constructs used in this study.

Antibodies, Immunoblot Analysis, and Immunoprecipitation—Total cell or tissue lysates were prepared in radioimmune precipitation assay buffer (150 mM NaCl, 1% Nonidet P-40, 0.1% sodium deoxycholate, 0.1% SDS, 100 mM Tris-HCl, pH 7.4) supplemented with protease inhibitors (Roche Applied Science). The lysates were cleared by centrifugation at 4 °C for 10 min at 10,000 × *g*. Protein concentration was determined using the Bradford assay (Bio-Rad) with bovine serum albumin as reference. The samples (10–40 μg) were separated on NuPAGE Bis-Tris gels (Invitrogen) and transferred to nitrocellulose. The membranes were probed with the following antibodies: LDLR (Cayman Chemical, 1:2000), tubulin (Calbiochem, 1:10000), GFP (affinity-purified rabbit polyclonal anti-GFP was a gift from Dr. Mireille Riedinger, 1:5000), LpR (2189/90, 1:500) (25), HA (Covance, 1:20000), V5 (Invitrogen, 1:5000), VLDLR (Santa Cruz clone 6A6, 1:250), α74 (1:20,000) (22), Reelin (Millipore clone G10, 1:200), Dab1 (D4 mouse monoclonal antibody was a gift from Dr. Andre Goffinet, 1:1000), and phosphotyrosine (Santa Cruz PY99, 1:200). Idol was detected with polyclonal antibodies raised in rabbits against Idol (13) or with a monoclonal antibody (Abcam, 1:500). Secondary horseradish peroxidase-conjugated antibodies (Zymed Laboratories Inc.) were used and visualized with chemiluminescence (Pierce). To immunoprecipitate HA-tagged proteins, equal amounts of protein of cleared lysates were incubated with EZ view red anti-HA affinity beads (Sigma) for 16 h. Subsequently, the beads were washed four times with radioimmune precipitation assay buffer. All of the incubations and washes were done at 4 °C with rotation. The proteins were eluted from the beads by boiling in 1× protein sample buffer for 5 min. The blots were quantified by densitometry.

RNA Isolation and Quantitative PCR—Total RNA was isolated from cells and mouse tissues using TRIzol (Invitrogen). One microgram of total RNA was reverse transcribed with random hexamers using iScript reverse transcription reagents kit (Bio-Rad). Sybergreen (Applied Biosystems) real time quantitative PCR assays were performed on an Applied Biosystems 7500HT sequence detector. The results show the averages of duplicate experiments normalized to 36B4. Primer sequences are available upon request.

Metabolic Labeling of Cells—HEK 293T cells were transfected with VLDLR-HA and Idol expression plasmids. Subsequently, the cells were washed twice with phosphate-buffered saline and pulsed for 15 min with Dulbecco's modified Eagle's medium lacking methionine and cysteine (Sigma) supplemented with 200 μCi/well easy Tag express ^{35}S protein labeling mix (PerkinElmer Life Sciences). The cells were then washed three times and chased in Dulbecco's modified Eagle's medium containing 10% fetal bovine serum, 100 μg/ml methionine, and 500 μg/ml cysteine for the indicated times. Preparation of cell lysates and immunoprecipitation of VLDLR-HA were conducted as detailed above.

Reelin Binding and Dab1 Phosphorylation Assays—Reelin binding assays were conducted essentially as described (22). Briefly, SNB19 cells were plated at a density of 0.5×10^6 cells/60-mm well. Subsequently, the cells were washed three times with Optimem medium (Invitrogen) and incubated with Reelin-containing conditioned medium on ice. Binding was allowed to proceed for 30 min, after which cells were vigorously washed five times with phosphate-buffered saline. Preparation of cell lysates and immunodetection was conducted as detailed above. Analysis of Dab1 phosphorylation following Reelin binding was done as described (22).

Animal Experiments—C57BL/6 mice (Jackson Laboratory) were fed a standard chow diet and housed in a temperature-controlled room under a 12-h light-dark cycle under pathogen-free conditions. The mice were orally gavaged with 20 mg/kg of the indicated LXR ligand. At the time of sacrifice, the tissues were collected, immediately frozen in liquid nitrogen, and stored at −80 °C. The tissues were processed for isolation of RNA and protein as above. The animal experiments were conducted in accordance with institutional guidelines.

Statistical Analysis—Real time PCR data and densitometry are expressed as the means ± S.D. Statistical analysis was done with a two-tailed Student's *t* test. A probability value of $p < 0.05$ was considered statistically significant.

RESULTS

The LXR Pathway Modulates the Levels of the VLDLR and ApoER2—We have recently shown that activation of LXRs diminishes LDLR protein levels and identified the E3 ubiquitin ligase Idol as the mediator of this effect (13). We therefore investigated whether other LDLR family members might be targets for the LXR-Idol pathway. We focused in particular on the most closely related proteins, VLDLR and ApoER2. Expression of these receptors is lost in most immortalized cell lines. However, inspection of the Biogps expression data revealed that glioblastoma cell lines express high levels of the *VLDLR*. We therefore tested the effect of two structurally unrelated LXR ligands on protein levels of this receptor. In SNB19 glioblastoma cells, we detect the VLDLR as two bands that likely represent the precursor and mature (fully glycosylated) receptor (Fig. 1*A*). Treatment of these cells with GW3965 or T0901317 increased the level of the LXR-responsive protein ABCA1 and concomitantly decreased the levels of the endogenous VLDLR (Fig. 1*A*). This reduction was not a result of decreased *VLDLR* expression. Whereas expression of the LXR target genes *ABCA1* and *IDOL* were increased, that of the

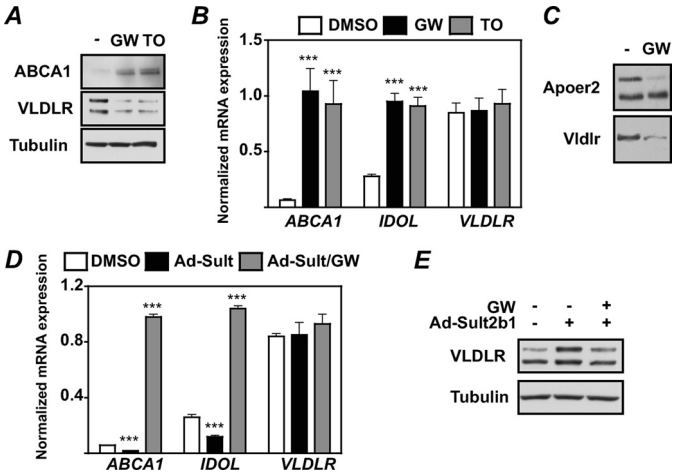

FIGURE 1. **The LXR pathway modulates the level of the VLDLR and ApoER2.** *A*, immunoblot analysis of total SNB19 cell lysates cells following treatment with 1 μM GW3965 (*GW*) or 1 μM T0901317 (*T0*) for 24 h. *B*, expression of *ABCA1*, *IDOL*, and *VLDLR* was analyzed in SNB19 cells treated for 24 h with 1 μM of the indicated ligand ($n = 4$). *C*, NIH-3T3 cells that stably produce either Vldlr or ApoER2 were treated for 24 h with 1 μM ligand. Subsequently, total cell lysates were analyzed by immunoblotting. *D*, gene expression was determined in SNB19 cells that were infected with the indicated adenoviruses for 24 h and subsequently treated for an additional 24 h as shown. *E*, immunoblot analysis of these cells ($n = 3$). The blots are representative of at least two independent experiments. The *bars* and *error bars* represent the means ± S.D. ***, $p < 0.001$. *DMSO*, dimethyl sulfoxide.

VLDLR remained unchanged (Fig. 1*B*). In similar studies, we also found that ligand-activated LXR decreased the level of VLDLR and APOER2 in 3T3 fibroblasts stably expressing these receptors (Fig. 1*C*) (22).

To investigate the link between endogenous LXR ligands and *VLDLR* expression, we utilized an adenovirus expressing oxysterol sulfotransferase (Sult2b1) (13, 23). Depletion of oxysterol LXR agonists by Sult2b1 in SNB19 cells decreased expression of LXR target genes as expected and had no effect on *VLDLR* expression (Fig. 1*D*). Nevertheless, this treatment increased VLDLR protein, and this effect was reversed by a synthetic LXR ligand (Fig. 1*E*). Cumulatively, these results suggest that LXR signaling can post-transcriptionally modulate the protein levels of the VLDLR and APOER2.

The reduced level of these receptors by activation of LXR was not limited to cells in culture but was also evident *in vivo*. Pharmacological dosing of mice with GW3965 led to induction of the LXR pathway in metabolic tissues without affecting *VLDLR* expression (Fig. 2*A*). Induction of *Idol* expression in these tissues was of a similar magnitude to that observed for the canonical LXR target gene *Abca1*. Concomitantly, we observed a decrease of VLDLR in skeletal muscle from these mice in response to LXR activation (Fig. 2, *B* and *C*). Conversely, we found that the level of Vldlr is increased in the brains of mice lacking LXRs (supplemental Fig. S1). Cumulatively, our results suggest that activation of LXR reduces protein levels of VLDLR and ApoER2 both *in vitro* and *in vivo* without affecting their transcript levels.

Idol Degrades the VLDLR and ApoER2—We have previously shown that the LXR-IDOL pathway targets the LDLR for degradation but not the related family members LRP1, SorLA, and LRP4 (13). Degradation by IDOL requires the presence of a highly conserved lysine residue that is adjacent to the NPVY

endocytosis motif present in the intracellular domain of the LDLR (Fig. 3*A*). Because this residue is highly conserved in the VLDLR and ApoER2, we tested whether IDOL underlies the LXR-mediated reduction of these receptors. In co-transfection experiments in HEK 293 cells, we found that both human and mouse IDOL reduce the level of the VLDLR and ApoER2, in addition to LDLR (Fig. 3*B*). Introducing an inactivating point mutation in the IDOL RING domain (C387A) (13) abrogated the effect on these receptors. Consistent with our previous studies of LDLR degradation, the most prominent effect of Idol was observed on the level of the mature (fully glycosylated) VLDLR and ApoER2 proteins. We confirmed that LXR requires Idol to reduce the levels of these receptors by knocking down Idol expression. A 70% reduction in Idol expression resulted in an increased basal level of VLDLR in 3T3-VLDLR cells and largely abrogated the ability of activated LXR to reduce the level of this receptor (supplemental Fig. S2). Unexpectedly, IDOL did not reduce the level of LRP1b, as may have been predicted based on sequence homology (Fig. 3, *A* and *B*) or the level of another NPVY-containing receptor, the epidermal growth factor receptor (data not shown). Our results further indicate that the substrate specificities of IDOL and PCSK9 overlap, because previous studies have suggested that PCSK9 can also reduce the protein levels of VLDLR and ApoER2 (26, 27).

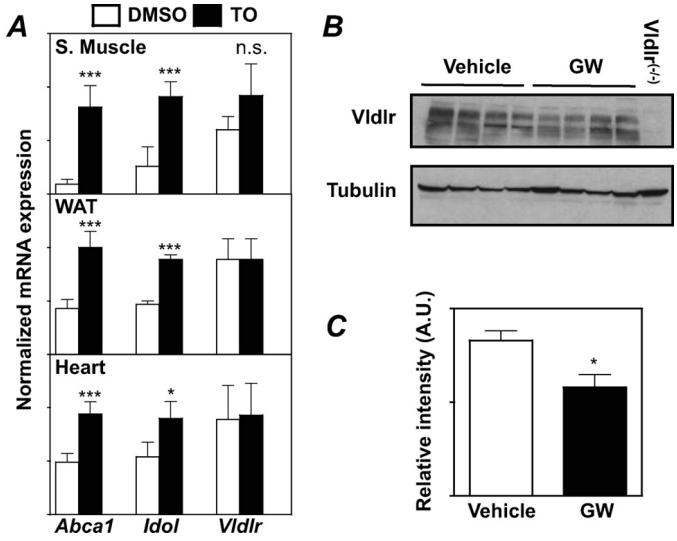

FIGURE 2. **The LXR-IDOL pathway modulates the level of the VLDLR *in vivo*.** *A*, C57Bl/6 mice ($n = 4–6$ mice/group) were orally gavaged for 3 days with the indicated ligand (20 mg/kg/day). Expression of *Abca1*, *Idol*, and *Vldlr* in several metabolic tissues was determined. *S. Muscle*, skeletal muscle; *WAT*, white adipose tissue. *B* and *C*, immunoblot analysis of Vldlr in skeletal muscle of C57Bl/6 mice pharmacologically dosed with an LXR ligand. The intensity of Vldlr was normalized to that of tubulin and is plotted. Skeletal muscle from a $Vldlr^{-/-}$ mouse was used as a negative control. The *bars* and *error bars* represent the means ± S.D. *, $p < 0.05$. *DMSO*, dimethyl sulfoxide; *GW*, GW3965; *T0*, T0901317.

The intracellular domain of the LDLR is critical for IDOL-dependent degradation. We have previously found that a mutant LDLR lacking the intracellular domain is resistant to IDOL-mediated degradation (13). We show here that replacing the natural intracellular domain of APP, which is not targeted by IDOL, with that of the LDLR allowed IDOL to target the chimeric receptor for destruction (Fig. 3*C*). This result demonstrates that the intracellular domain is both necessary and sufficient to direct Idol-dependent degradation of plasma membrane proteins.

The function of members of the LDLR family of receptors is evolutionarily conserved. Accordingly, we find that IDOL degrades the LpR, an ancient LDLR-related receptor from the migrating locust (*Locusta migratoria*) that is important for lipoprotein uptake in this species (Fig. 3, *A* and *D*) (25). We next asked the reciprocal question of whether the function of IDOL itself is evolutionarily conserved. We identified IDOL homologs in both vertebrate and nonvertebrate species (supplemental Fig. S3). The *D. melanogaster* Dnr1 gene is a distant homolog of mammalian IDOL (28). Remarkably, Dnr1 degraded the human LDLR and VLDLR dependent on an intact RING domain (Fig. 3*E*). Dnr1 is an inhibitor of the inflammatory IMD pathway in flies (28). However, despite the fact that both Dnr1 and IDOL degrade the LDLR and VLDLR, IDOL was unable to inhibit the IMD pathway in S2 cells (supplemental Fig. S4). In conclusion, these results suggest that the ability of IDOL to degrade members of the LDLR family is an evolutionarily conserved mechanism to modulate lipoprotein uptake.

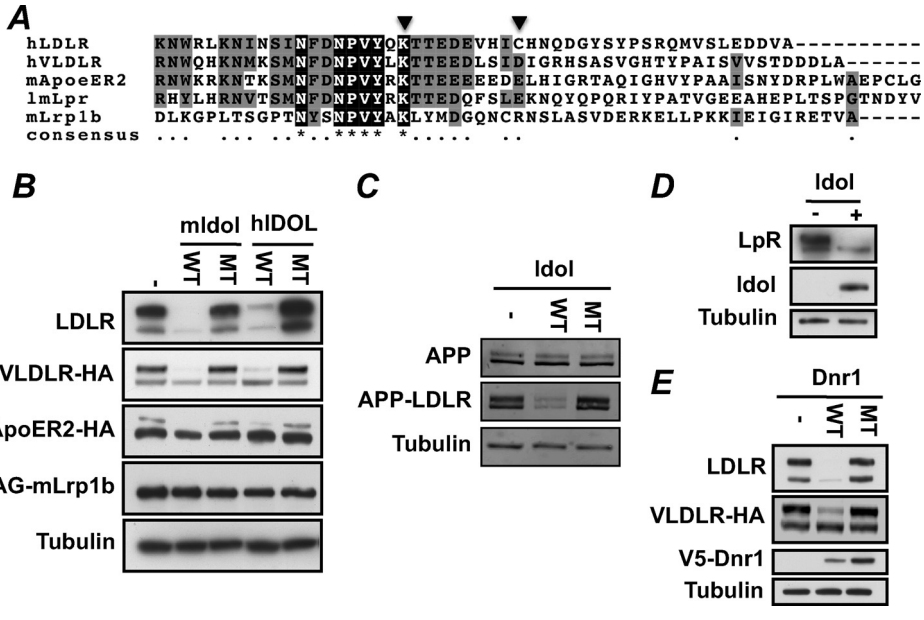

FIGURE 3. **IDOL targets the LDLR, VLDLR, and ApoER2 for degradation and is evolutionarily conserved.** *A*, alignment of the intracellular domains of the human (*h*) LDLR, human VLDLR, mouse (*m*) ApoER2, *L. migratoria* LpR (*lmLpr*), and mouse Lrp1b. The *triangles* represent the conserved lysine following the NPVY endocytic motif and the cysteine that is ubiquitinated in the LDLR (13). The ApoER2 sequence is cut because of space considerations. *B–E*, HEK 293T cells were co-transfected with the indicated plasmids, and the total cell lysates were analyzed by immunoblotting as indicated. *WT*, wild type; *MT*, mutant. The blots are representative of at least two independent experiments.

Post-translational Degradation of the VLDLR by Idol—Activation of the LXR pathway leads to decreased levels of VLDLR and ApoER2 protein without an effect on the respective transcript (Fig. 1, *A–C*, and not shown). Adenoviral expression of Idol in SNB19 cells had a similar effect (Fig. 4*A*). These findings are consistent with a post-translational effect on receptor levels. Pulse-chase metabolic labeling experiments revealed that Idol did not impact the translation of the VLDLR (Fig. 4*B*). In the absence of Idol, the VLDLR rapidly matures as evidenced by the appearance of a lower mobility band representing the fully glycosylated receptor. Idol expression prevented the appearance of the mature form of the receptor, consistent with our prior observations with the LDLR.

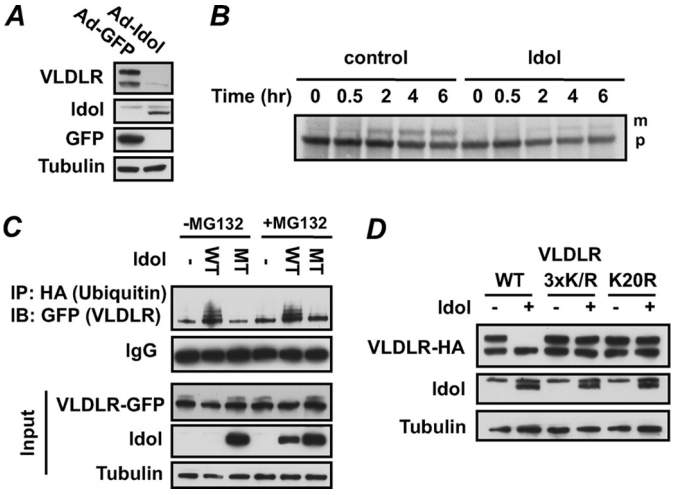

FIGURE 4. **Post-translations regulation of the VLDLR by IDOL is dependent on ubiquitination of a single conserved lysine residue.** *A*, adenovirally mediated expression of Idol in SNB19 cells leads to a decreased level of endogenous Vldlr. *B*, HEK 293T cells were co-transfected with a VLDLR and a control or Idol expression plasmid. 48 h after transfection cells were pulsed with [^{35}S]methionine and [^{35}S]cysteine for 15 min and chased as indicated. The samples were immunoprecipitated (*IP*) at the indicated time points after labeling. *p* and *m* represent the precursor and mature VLDLR protein, respectively. *C*, HEK 293T cells were co-transfected with VLDLR-GFP, Idol, and HA-ubiquitin expression plasmids as indicated. Subsequently, the cells were treated with vehicle or 25 μM MG132 for 6 h. *D*, HEK 293T cells were co-transfected with Idol and wild type or mutant VLDLR-HA expression plasmids. Total cell lysates were analyzed by immunoblotting (*IB*). The blots are representative of at least two independent experiments.

Because Idol is an E3 ubiquitin-ligase, we tested whether the VLDLR was ubiquitinated by Idol. In the presence of active Idol, we observed the appearance of polyubiquitinated VLDLR (Fig. 4*C*). Pharmacological blocking of the proteosome did not result in increased ubiquitination of the VLDLR and did not impair degradation of the receptor by Idol (Fig. 4*C*). Blocking lysosomal function with the lysosomotropic agents ammonium chloride or chloroquine, on the other hand, largely inhibited the LXR-mediated reduction of Vldlr abundance (supplemental Fig. S5). These observations are consistent with Idol-dependent lysosomal degradation of the VLDR as we recently proposed for the LDLR (13).

Having established that the VLDLR is subject to ubiquitination by Idol, we next attempted to identify the target residue(s). Mutation of all three lysine residues present in the intracellular tail of the VLDLR abolished degradation by Idol (Fig. 4*D*). Remarkably, mutating the highly conserved lysine residue immediately following the NPVY endocytotic motif resulted in the same outcome, indicating that this residue is the sole target for Idol-mediated ubiquitination. Note that the cysteine residue that serves as a second target for Idol in the LDLR is not conserved in either the VLDLR or ApoER2 (Fig. 3*A*).

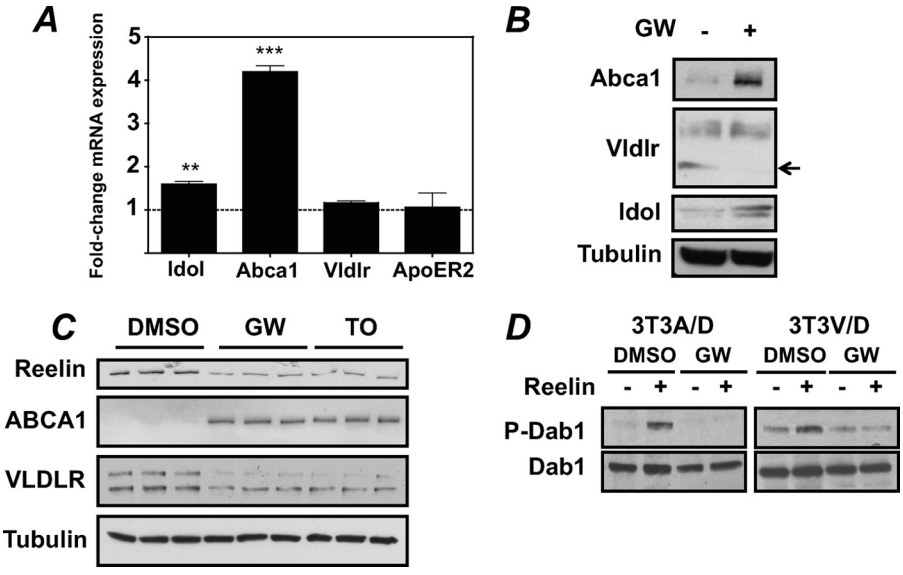

FIGURE 5. **Functional cross-talk between the LXR pathway and Reelin signaling.** *A*, gene expression analysis of primary rat hippocampal neurons treated with 1 μM GW3965 (*GW*) ligand for 24 h. The fold change in mRNA expression following GW treatment is plotted. Expression of the indicated genes in dimethyl sulfoxide-treated cells (*DMSO*) was set to 1 (n = 4–6). *B*, immunoblot analysis of primary rat hippocampal neurons treated with 1 μM GW ligand for 24 h. The *arrow* indicates the Vldlr isoform that is modulated by LXR treatment (n = 4–6). *C*, SNB19 cells were treated with 1 μM of the indicated LXR ligands or dimethyl sulfoxide for 24 h. Subsequently, binding of Reelin to the cells and the level of the indicated proteins were determined by immunoblotting (n = 3). *D*, NIH 3T3 cells that stably produce Dab1 and VLDLR (3T3V/D) or ApoER2 (3T3A/D) were treated with or without 1 μM GW and Reelin or mock conditioned media as indicated. The level of total Dab1 and phospho-Dab1 were determined by immunoblotting. The blots are representative of at least two independent experiments. The *bars* and *error bars* represent the means ± S.D. **, $p < 0.01$; ***, $p < 0.001$. *T0*, T0901317.

The LXR-IDOL Axis Reduces Reelin Binding and Dab1 Phosphorylation—In addition to their proposed roles in metabolism, the VLDLR and ApoER2 are critical for neuronal migration during development (16, 20, 21). We therefore asked whether the LXR-IDOL pathway was functional in neurons. Treatment of primary rat neurons with an LXR ligand increased the mRNA and protein levels of Abca1 and Idol, whereas expression of *Vldlr* did not change (Fig. 5*A*). Given the fact that it is an unstable protein, detection of endogenous Idol expression has been difficult (13). Interestingly, this is the first observation that activation of LXR increases the level of endogenous Idol protein. Several isoforms of the VLDLR have been observed in neurons (26, 29). We found that the isoform lacking the *O*-linked glycosyla-

tion domain, which runs with higher mobility in these cells, was most dramatically decreased in response to LXR activation (Fig. 5*B* and supplemental Fig. S6). Notably, this is similar to what was observed for Pcsk9 (26).

An expected consequence of reduced VLDLR expression in neurons would be decreased Reelin binding and signaling. We initially chose SNB19 cells as a cellular model to test this possibility. Activation of the LXR pathway in these cells with the two different ligands GW3965 and T0901317 decreased the level of the VLDLR to 26 ± 4 or 22 ± 8% of the control treated cells, respectively (Fig. 5*C*). Furthermore, this was mirrored by a decrease in Reelin binding. To test whether this also led to decreased Dab1 phosphorylation, we used 3T3 cells that had been stably reconstituted with VLDLR or ApoER2 and with Dab1 (22). Functionally, these cells responded to Reelin in a similar fashion to primary neurons, with Reelin binding strongly stimulating Dab1 phosphorylation (Fig. 5*D*). Activation of LXR in these cells largely blocked this Reelin-dependent effect but had no influence on total Dab1 levels (Fig. 5*D*). Thus, the ability of LXR to modulate the levels of the neuronal lipoprotein receptors VLDLR and ApoER2 appears to have a functional consequence for Reelin signaling.

DISCUSSION

In this study we demonstrate that, in addition to modulating the LDLR, the LXR pathway also post-translationally regulates the levels of the related receptors VLDLR and ApoER2. Mechanistically, this is the result of transcriptional induction of the E3 ubiquitin ligase IDOL that targets these receptors for lysosomal degradation. The ability of the LXR-IDOL pathway to target multiple members of the LDLR superfamily suggests a potential role for this pathway in processes beyond lipid metabolism.

Over the last decade the role of LXR in peripheral cholesterol and energy metabolism has been the subject of considerable research interest (30). However, it has recently become apparent that LXRs also play important roles in maintaining cholesterol homeostasis and attenuating inflammatory events in the CNS. Accordingly, the LXR pathway in the CNS has been proposed to be a potential target for treatment of Alzheimer disease (31–33), Nieman-Pick C (34), and ischemic events (35, 36). Our current study extends the possible roles for LXR in the CNS. IDOL is expressed in neurons and is induced by LXR agonists in these cells both at the mRNA and protein levels. In these cells IDOL has been proposed to inhibit neurite outgrowth (37) and, as we show here, to modulate the Reelin pathway by controlling the levels of VLDLR and ApoER2. Reelin interaction with the VLDLR and ApoER2 is critical during development because it properly directs the positioning of neurons (16, 20, 21). Because only the combined loss of both receptors results in severely impaired neuronal positioning (16), the ability of IDOL to simultaneously target both receptors for degradation may allow it to modulate this pathway. Whether IDOL does this *in vivo* is unknown. Intriguingly, despite having a similar Reelin level, mice lacking LXR display disrupted neuronal migration, which Fan *et al.* (38) attributed to a reduction in the number of vertical processes emanating from the radial glia cells. Because the formation of vertical processes emanating from these cells requires proper Reelin signaling (39) and the LXR null mice have substantially reduced Idol expression (13), it remains to be seen whether Idol contributes to the observed migratory defect. Furthermore, the phosphorylation of Dab1 downstream of the VLDLR and ApoER2 is not limited to the CNS. In macrophages, ligation of ApoER2 by activated protein C results in Dab1-dependent signaling events (40). This raises the possibility that the LXR-IDOL pathway may be involved not only in Reelin signaling in the CNS but also in peripheral Dab1-dependent processes.

Our investigation of the substrate specificity of IDOL was largely prompted by the high degree of evolutionary conservation within the LDLR family of receptors (14). Of the mammalian members tested, only the LDLR, VLDLR, and ApoER2 appear to be IDOL targets. Remarkably, IDOL was also able to degrade an ancient LDLR family member important for lipoprotein uptake in the migrating locust. IDOL itself is also highly evolutionarily conserved, with homologs found in both vertebrates and nonvertebrates. The *D. melanogaster* Dnr1 gene is a highly divergent homolog of mammalian IDOL (28). Nevertheless, Dnr1 degraded the LDLR and VLDLR in co-transfection assays in a RING-dependent manner. Dnr1 has been reported to inhibit the IMD pathway in flies. This pathway is important for the innate response to Gram-negative bacteria in flies and shares similarities with the mammalian tumor necrosis factor cascade. Dnr1 inhibits the IMD pathway by blocking the activity of the fly caspases-8 homolog, Dredd (41). However, our data indicate that IDOL was unable to attenuate the IMD pathway when stably expressed in S2 macrophage-like cells, suggesting that this capacity has been lost during evolution. A plausible explanation for this lies in the fact that the region in Dnr1 identified as crucial for interaction with Dredd is absent in IDOL (41).

The delineated substrate specificity allows us to also further define the structural requirements for receptor recognition by IDOL. The intracellular domain of the LDLR forms a scaffold for protein-protein interactions essential for proper function and trafficking of the receptor (42). Furthermore, this domain is both required and sufficient for recognition by IDOL. This implies that all of the IDOL recognition determinants are encoded within this region. Sequence comparison of the receptors targeted by IDOL reveals that a limited region surrounding the NPVY endocytosis motif is highly conserved. The lysine residue following this motif is essential for ubiquitination by IDOL (Ref. 13 and Fig. 4*D*). However, its presence is not sufficient, because LRP1b is not targeted by IDOL. Future identification of the putative IDOL/receptor interaction interface may facilitate development of structure-based inhibitors aimed specifically at disrupting the IDOL-LDLR association. Such inhibitors would be predicted to increase the level of the LDLR and may complement statins for treating hypercholesterolemia.

Similar to IDOL, the secreted protein PCSK9 also post-translationally modulates the levels of the LDLR, VLDLR, and ApoER2 (26, 27). The overlapping substrate specificities of IDOL and PCSK9 raise the intriguing possibility that they act in a concerted fashion. It is highly unlikely that these two proteins directly interact. PCSK9 is a secreted protein that binds the ecto-domain of the receptors and promotes their endocytosis

and lysosomal degradation. It has also been recently proposed that PCSK9 can act on the LDLR within the cell (43). IDOL, on the other hand, recognizes the intracellular tail of these receptors. It remains to be seen whether these two proteins functionally cooperate to regulate the level of these receptors and, if so, whether this occurs during their maturation or subsequent to their endocytosis. Of note, under several conditions the activity of IDOL on the LDLR seems to be independent of PCSK9. IDOL degrades the LDLR in cells that do not express PCSK9 (*e.g.* macrophages) as well as endocytosis mutants of the LDLR, VLDLR, and ApoER2. Clearly, further studies to clarify the functional relationship between PCSK9 and IDOL are required.

In conclusion, we demonstrate here that the LXR-IDOL pathway targets the VLDLR and ApoER2 for degradation. This suggests that in addition to potential roles in metabolism, IDOL may also have a role in neurons during development.

Acknowledgments—We thank the members of our laboratories for fruitful discussions. We especially acknowledge the suggestions of Carlie de Vries, Hans Aerts, Arthur Verhoeven, Boris Bleijlevens, and Irith Koster for critically reading the manuscript. We thank David Russell for the Sult2b1 adenovirus.

REFERENCES

1. Russell, D. W., Schneider, W. J., Yamamoto, T., Luskey, K. L., Brown, M. S., and Goldstein, J. L. (1984) *Cell* **37,** 577–585
2. Hobbs, H. H., Russell, D. W., Brown, M. S., and Goldstein, J. L. (1990) *Annu. Rev. Genet.* **24,** 133–170
3. Tolleshaug, H., Hobgood, K. K., Brown, M. S., and Goldstein, J. L. (1983) *Cell* **32,** 941–951
4. Brown, M. S., and Goldstein, J. L. (1986) *Science* **232,** 34–47
5. Yokoyama, C., Wang, X., Briggs, M. R., Admon, A., Wu, J., Hua, X., Goldstein, J. L., and Brown, M. S. (1993) *Cell* **75,** 187–197
6. Hua, X., Yokoyama, C., Wu, J., Briggs, M. R., Brown, M. S., Goldstein, J. L., and Wang, X. (1993) *Proc. Natl. Acad. Sci. U.S.A.* **90,** 11603–11607
7. Goldstein, J. L., DeBose-Boyd, R. A., and Brown, M. S. (2006) *Cell* **124,** 35–46
8. Garcia, C. K., Wilund, K., Arca, M., Zuliani, G., Fellin, R., Maioli, M., Calandra, S., Bertolini, S., Cossu, F., Grishin, N., Barnes, R., Cohen, J. C., and Hobbs, H. H. (2001) *Science* **292,** 1394–1398
9. Abifadel, M., Varret, M., Rabès, J. P., Allard, D., Ouguerram, K., Devillers, M., Cruaud, C., Benjannet, S., Wickham, L., Erlich, D., Derré, A., Villéger, L., Farnier, M., Beucler, I., Bruckert, E., Chambaz, J., Chanu, B., Lecerf, J. M., Luc, G., Moulin, P., Weissenbach, J., Prat, A., Krempf, M., Junien, C., Seidah, N. G., and Boileau, C. (2003) *Nat. Genet.* **34,** 154–156
10. Cohen, J., Pertsemlidis, A., Kotowski, I. K., Graham, R., Garcia, C. K., and Hobbs, H. H. (2005) *Nat. Genet.* **37,** 161–165
11. Maxwell, K. N., and Breslow, J. L. (2004) *Proc. Natl. Acad. Sci. U.S.A.* **101,** 7100–7105
12. Park, S. W., Moon, Y. A., and Horton, J. D. (2004) *J. Biol. Chem.* **279,** 50630–50638
13. Zelcer, N., Hong, C., Boyadjian, R., and Tontonoz, P. (2009) *Science* **325,** 100–104
14. Herz, J., and Bock, H. H. (2002) *Annu. Rev. Biochem.* **71,** 405–434
15. Tacken, P. J., Hofker, M. H., Havekes, L. M., and van Dijk, K. W. (2001) *Curr. Opin. Lipidol.* **12,** 275–279
16. Trommsdorff, M., Gotthardt, M., Hiesberger, T., Shelton, J., Stockinger, W., Nimpf, J., Hammer, R. E., Richardson, J. A., and Herz, J. (1999) *Cell* **97,** 689–701
17. Sheldon, M., Rice, D. S., D'Arcangelo, G., Yoneshima, H., Nakajima, K., Mikoshiba, K., Howell, B. W., Cooper, J. A., Goldowitz, D., and Curran, T. (1997) *Nature* **389,** 730–733
18. Howell, B. W., Hawkes, R., Soriano, P., and Cooper, J. A. (1997) *Nature* **389,** 733–737
19. Hirotsune, S., Takahara, T., Sasaki, N., Hirose, K., Yoshiki, A., Ohashi, T., Kusakabe, M., Murakami, Y., Muramatsu, M., Watanabe, S., Nakao, K., Katsuki, M., and Hayashizaki, Y. (1995) *Nat. Genet.* **10,** 77–83
20. Hiesberger, T., Trommsdorff, M., Howell, B. W., Goffinet, A., Mumby, M. C., Cooper, J. A., and Herz, J. (1999) *Neuron* **24,** 481–489
21. D'Arcangelo, G., Homayouni, R., Keshvara, L., Rice, D. S., Sheldon, M., and Curran, T. (1999) *Neuron* **24,** 471–479
22. Mayer, H., Duit, S., Hauser, C., Schneider, W. J., and Nimpf, J. (2006) *Mol. Cell. Biol.* **26,** 19–27
23. Chen, W., Chen, G., Head, D. L., Mangelsdorf, D. J., and Russell, D. W. (2007) *Cell Metab.* **5,** 73–79
24. Sokka, A. L., Putkonen, N., Mudo, G., Pryazhnikov, E., Reijonen, S., Khiroug, L., Belluardo, N., Lindholm, D., and Korhonen, L. (2007) *J. Neurosci.* **27,** 901–908
25. Van Hoof, D., Rodenburg, K. W., and Van der Horst, D. J. (2002) *J. Cell Sci.* **115,** 4001–4012
26. Poirier, S., Mayer, G., Benjannet, S., Bergeron, E., Marcinkiewicz, J., Nassoury, N., Mayer, H., Nimpf, J., Prat, A., and Seidah, N. G. (2008) *J. Biol. Chem.* **283,** 2363–2372
27. Shan, L., Pang, L., Zhang, R., Murgolo, N. J., Lan, H., and Hedrick, J. A. (2008) *Biochem. Biophys. Res. Commun.* **375,** 69–73
28. Foley, E., and O'Farrell, P. H. (2004) *PLoS Biol.* **2,** E203
29. Sakai, K., Tiebel, O., Ljungberg, M. C., Sullivan, M., Lee, H. J., Terashima, T., Li, R., Kobayashi, K., Lu, H. C., Chan, L., and Oka, K. (2009) *Brain Res.* **1276,** 11–21
30. Zelcer, N., and Tontonoz, P. (2006) *J. Clin. Invest.* **116,** 607–614
31. Jiang, Q., Lee, C. Y., Mandrekar, S., Wilkinson, B., Cramer, P., Zelcer, N., Mann, K., Lamb, B., Willson, T. M., Collins, J. L., Richardson, J. C., Smith, J. D., Comery, T. A., Riddell, D., Holtzman, D. M., Tontonoz, P., and Landreth, G. E. (2008) *Neuron* **58,** 681–693
32. Koldamova, R. P., Lefterov, I. M., Staufenbiel, M., Wolfe, D., Huang, S., Glorioso, J. C., Walter, M., Roth, M. G., and Lazo, J. S. (2005) *J. Biol. Chem.* **280,** 4079–4088
33. Zelcer, N., Khanlou, N., Clare, R., Jiang, Q., Reed-Geaghan, E. G., Landreth, G. E., Vinters, H. V., and Tontonoz, P. (2007) *Proc. Natl. Acad. Sci. U.S.A.* **104,** 10601–10606
34. Repa, J. J., Li, H., Frank-Cannon, T. C., Valasek, M. A., Turley, S. D., Tansey, M. G., and Dietschy, J. M. (2007) *J. Neurosci.* **27,** 14470–14480
35. Morales, J. R., Ballesteros, I., Deniz, J. M., Hurtado, O., Vivancos, J., Nombela, F., Lizasoain, I., Castrillo, A., and Moro, M. A. (2008) *Circulation* **118,** 1450–1459
36. Sironi, L., Mitro, N., Cimino, M., Gelosa, P., Guerrini, U., Tremoli, E., and Saez, E. (2008) *FEBS Lett.* **582,** 3396–3400
37. Olsson, P. A., Korhonen, L., Mercer, E. A., and Lindholm, D. (1999) *J. Biol. Chem.* **274,** 36288–36292
38. Fan, X., Kim, H. J., Bouton, D., Warner, M., and Gustafsson, J. A. (2008) *Proc. Natl. Acad. Sci. U.S.A.* **105,** 13445–13450
39. Hartfuss, E., Förster, E., Bock, H. H., Hack, M. A., Leprince, P., Luque, J. M., Herz, J., Frotscher, M., and Götz, M. (2003) *Development* **130,** 4597–4609
40. Yang, X. V., Banerjee, Y., Fernández, J. A., Deguchi, H., Xu, X., Mosnier, L. O., Urbanus, R. T., de Groot, P. G., White-Adams, T. C., McCarty, O. J., and Griffin, J. H. (2009) *Proc. Natl. Acad. Sci. U.S.A.* **106,** 274–279
41. Primrose, D. A., Chaudhry, S., Johnson, A. G., Hrdlicka, A., Schindler, A., Tran, D., and Foley, E. (2007) *J. Cell Sci.* **120,** 1189–1199
42. Gotthardt, M., Trommsdorff, M., Nevitt, M. F., Shelton, J., Richardson, J. A., Stockinger, W., Nimpf, J., and Herz, J. (2000) *J. Biol. Chem.* **275,** 25616–25624
43. Poirier, S., Mayer, G., Poupon, V., McPherson, P. S., Desjardins, R., Ly, K., Asselin, M. C., Day, R., Duclos, F. J., Witmer, M., Parker, R., Prat, A., and Seidah, N. G. (2009) *J. Biol. Chem.* **284,** 28856–28864